Theoretical interpretation of the vacuum ultraviolet reflectance of liquid helium and of the absorption spectra of helium microbubbles in aluminum

A. A. Lucas, J. P. Vigneron, and S. E. Donnelly
Institute for Research in Interface Sciences, Facultés Universitaires Notre-Dame de la Paix, B-5000 Namur, Belgium

J. C. Rife
Naval Research Laboratory, Washington, D.C. 20375
(Received 26 October 1982)

The position and width of the helium resonance line $1^1S_0 \rightarrow 2^1P_1$ are calculated for a high-density helium fluid. The theory aims at understanding the reflectivity data of Surko *et al.* for the low-temperature liquid-vapor interface and the absorption data of Rife *et al.* for room-temperature, high-pressure helium bubbles in aluminum. The theoretical ingredients of the model are (i) the long-range dipole interaction of an excited $2P$ atom with the rest of the fluid and with the metal substrate; (ii) the short-range Pauli pseudorepulsion arising from orthogonalization of the $2p$-electron wave function with the $1s$ ground-state orbital of neighboring atoms; (iii) a statistical treatment of the high-density fluid based either on the experimentally measured radial pair distribution function of low-T liquid He, or on the Percus-Yevick distribution function of hard spheres and the theoretical equation of state of Young *et al.* for the He fluid in the bubbles; (iv) the standard static line-broadening theory to calculate the effect of Pauli repulsion on the line shapes. The theory provides a reasonably accurate understanding of the observed spectra in both the liquid and high-density gas, and can serve as a sound basis for interpretation of vacuum ultraviolet spectra in other gas-metal combinations.

I. INTRODUCTION

Investigations by means of vacuum ultraviolet (vuv) absorption and electron-energy-loss spectroscopy[1-3] (EELS) of helium-implanted aluminum films have been conducted in the last few years with the aim of obtaining information on the density of helium in the bubbles which develop as a result of the implantation. One major result of this work was that the He resonance line which occurs at 21.22 eV (584.3 Å) in the dilute gas was observed to shift towards higher energies and to broaden by varying amounts, depending on experimental conditions. Typically, samples containing 1.45 at.% He in a fairly uniform distribution of bubble sizes (50±10 Å diam) had an absorption band peaked at 22.6 eV and broadened to 1.2 eV. More heavily implanted samples with an average of 3.5 at.% He had higher shift (2 eV) and larger width (2.2 eV).[2]

The qualitative interpretation proposed in Ref. 2 for such large shift and broadening was in terms of an inhomogeneous raising of the atomic $2P$ level as due to a cage effect produced around the excited atom by the coordinating ground-state atoms. An identical argument was invoked by Surko *et al.*[4] to interpret their observation of a small blue shift of the resonance line as measured from the reflectivity of the low-temperature liquid. The cage effect stems from the Pauli pseudopotential repulsion brought about by the orthogonalization of the $2p$ wave function with the $1s^2$ closed-shell orbital of ground-state He atoms.

Other shift and broadening mechanisms were studied previously by Ohtaka and Lucas.[5] They concluded that for bubble radii larger than a few Å, the dipole resonance effect should make a nonnegligible density-dependent contribution to the overall line shape. This mechanism will be reviewed (Sec. II) as it bears on the interpretation of the spectrum at densities corresponding to the liquid.

The principal aim of the present work (Secs. III and IV) is to make a quantitative study of the Pauli repulsion effect which was only sketched in Ref. 2. The model proposed here incorporates a good description of the perturbation of the dense fluid on the electronic structure of excited He and, moreover, takes account of the statistical structure of the fluid itself. We arrive at the following main conclusions:

(1) At the *lower end of the density scale* the line shape in a macroscopic gas sample is governed by the usual red-shifting dipole resonance effect. This mechanism, which depends linearly on density, can

be qualified as of long range due to the *long-range* nature of the dipole interaction. When the gas sample is enclosed in a metal cavity of microscopic dimensions (smaller than the resonance wavelength), the resonance shift is largely canceled by the depolarizing effect of the metal-cavity surface.

(2) *At high density,* the line shape is dominated by the blue-shifting Pauli repulsion effect. This is a *short-range* mechanism, originating from orthogonalization of localized wave functions.

(3) *The cryogenic liquid* has a density for which short- and long-range effects are of comparable size, giving a net weak blue shift of the resonance line.

(4) *The large blue shifts* observed in our He-Al samples are indicative of densities 2 to 5 times the liquid density.

The model study proposed here is intended to be a useful contribution towards establishing the vuv and EELS spectroscopic techniques as powerful quantitative tools for investigation of other gas-metal combinations of interest in material technology.

II. DIPOLE RESONANCE EFFECT

The feasibility of investigating the He-Al system by means of ultraviolet absorption and EELS was evaluated a few years ago.[5] It was thought in this work, before the experiment could be performed, that the leading effect would be the dipole resonance shift and broadening which usually dominate the line shape of a dipole-allowed transition in a pure gas at low and moderate pressures.

The resonance effect arises from the fact that an optical excitation of one atom may transfer resonantly to neighboring atoms through the dipole-dipole interaction. Let n be the number density and let ω_0 be the resonance frequency that the atoms would have, at that density, if the dipole-dipole interaction was turned off. Thus ω_0 possibly includes other shifts operating at the indicated density. For the purpose of obtaining the further perturbation suffered by the atomic frequency due to the dipolar interaction, it is sufficient to analyze the dielectric properties of the fluid in terms of the Clausius-Mosotti formula for the dielectric function

$$\epsilon(\omega)=1+4\pi n\alpha(\omega)\left[1-\frac{4\pi}{3}n\alpha(\omega)\right]^{-1}, \qquad (1)$$

where $\alpha(\omega)$ is the He ground-state polarizability at frequency ω. Let us indeed recall that the denominator in (1) arises from dipole-dipole interactions and takes proper account of the red-shifting effect of the dipole Lorentz field on the position of the individual atomic lines making up $\alpha(\omega)$. Neglecting this effect (as apparently was done in the analysis of Ref. 4) results in underestimating the net blue shift of the liquid resonance line with respect to the unperturbed atomic transition.

On account of the large $1S\rightarrow 2P$ dipole oscillator strength of He we begin by simulating $\alpha(\omega)$, in the vicinity of $\omega=\omega_0$, by just two Lorentzian lines,

$$\alpha(\omega)=\frac{e^2}{m}\frac{f_0}{\omega_0^2-\omega^2-i\omega\gamma_0}+\frac{e^2}{m}\frac{f_R}{\omega_R^2-\omega^2}, \qquad (2)$$

where f_0, and f_R are oscillator strengths and γ_0 is the width of the resonance line in the fluid.

The second oscillator in Eq. (2) mimics the remainder of the spectrum. Of the five parameters of this model, only the first three ω_0, f_0, and γ_0 may be varied independently to fit the optical properties around ω_0. Indeed, f_R and ω_R are determined from f_0 and ω_0 by requiring that (i) the sum rule $f_0+f_R=2$ should hold, and (ii) the quasistatic polarizability of He as measured in the visible for high-density gas[6] should be $\alpha(0)\simeq 0.205$ Å^3.

The (near-normal) reflectivity function[7] $R(\omega)=|1-\sqrt{\epsilon}|^2/|1+\sqrt{\epsilon}|^2$ can be calculated from (1) and (2) at liquid-He density and compared with the experimental reflectivity data.[4] An excellent fit to the data (within a few percent) in peak position, height, and width was found for the following values of the parameters: $f_0=0.49$, $\hbar\omega_0=21.61$ eV, and $\hbar\gamma_0=0.43$ eV. Thus the resonance line at that density appears to be blue shifted by 0.38 eV (Ref. 4 estimated 0.2 eV only due to the neglect of the Lorentz field effect) and broadened to 0.43 eV [full width at half maxium (FWHM)].

Improvement of the model has been achieved by performing a Kramers-Kronig (KK) analysis of the data of Surko *et al.*[4] The latter being given in a narrow energy range ($19.5<\hbar\omega<24$ eV), it is necessary to extrapolate the wings of the resonance spectrum by fitting oscillators to the reflectivity R and its derivative $dR/d\omega$ at each end of the data range. In the low-energy wing this was done with the following oscillators:

$$\hbar\omega_0=21.61,\quad f_0=0.51,\quad \hbar\gamma_0=0.47, \qquad (3)$$

$$\hbar\omega_1=24,\quad f_1=0.32,\quad \hbar\gamma_1=2, \qquad (4)$$

where $\hbar\omega_0$, $\hbar\gamma_0$, $\hbar\omega_1$, and $\hbar\gamma_1$ are measured in eV, respectively. The summed oscillators give a real part of the refractive index $n=1.026$ at $\hbar\omega=2.5$ eV, which is in close agreement with the observed value of $n=1.025$.[8] Note that the required strength $f_0\simeq 0.5$ in both the two-oscillator model (2) and in the present KK analysis is substantially higher than the free-atom value $f_{1S\rightarrow 2P}=0.276$. On the high-energy side of the resonance line, the extrapolation was achieved by adding to the line (4) a broad peak

$$\hbar\omega_2=35,\ f_2=1.86\ ,\ \hbar\gamma_2=50\ , \tag{5}$$

where $\hbar\omega_2$ and $\hbar\gamma_2$ are measured in eV, respectively. This yielded reasonable results for the magnitude and falloff of the imaginary part k of the refractive index relative to the measured atomic photoionization cross section at high energy.[9] In addition, with these extrapolations the ϵ_2 sum rule for the effective number of electrons participating to absorption at energy E saturates at the nearly correct value at high energy (2.08 instead of 2, see Fig. 4).

Optical constants obtained from the KK inversion are plotted in Figs. 1–4. Table I gives the resonance-peak parameters in the various optical functions R, k, α, and ϵ_2. From these results it must be concluded that in the cryogenic liquid, the He resonance absorption has been blue shifted and broadened by a further interaction mechanism which will be investigated in Sec. III.

The analysis given above applies if the dimensions of the fluid sample are much larger than the wavelength (584 Å). When the He gas is bounded in a small cavity of the metal, the depolarizing factor of the metal boundary modifies these results. The finite-size effect has been considered in Ref. 5 from the point of view of a standard effective-medium theory.[10] When, as in our case, the bubble size is smaller than the wavelength, the effective dielectric function of the He-Al composite medium is given by

$$\bar{\epsilon}(\omega)=\epsilon_m(\omega)+3f\frac{\epsilon_m(\epsilon_g-\epsilon_m)}{\epsilon_g+2\epsilon_m}\ , \tag{6}$$

where ϵ_m and ϵ_g are the Al-metal and the He-gas dielectric functions, and where f is the ratio of bubble volume to total volume. For (6) to be valid, f must be small, e.g., under 10%, and the bubbles should be spherical. Both conditions are realized in many of our samples. Otherwise more complicated forms of $\bar{\epsilon}$ are available which allow for arbitrary filling fraction f or more general bubble shapes.[10]

In the neighborhood of the He resonance line, ϵ_m is nearly constant[11] at $\epsilon_m\simeq 0.5+0.03i$, whereas $\epsilon_g(\omega)$ has the Lorentzian shape of Eqs. (1) and (2). f being small, we can approximate the absorption coefficient by

$$\begin{aligned}\mathrm{Im}\sqrt{\bar{\epsilon}}&\simeq\mathrm{Im}\left[\sqrt{\epsilon_m}\left[1+\tfrac{3}{2}f\frac{\epsilon_g-\epsilon_m}{\epsilon_g+2\epsilon_m}\right]\right]\\&=\tfrac{3}{2}f(\mathrm{Re}\sqrt{\epsilon_m})\mathrm{Im}\frac{\epsilon_g-\epsilon_m}{\epsilon_g+2\epsilon_m}\ .\end{aligned} \tag{7}$$

The imaginary-part factor has a Lorentzian shape peaked at the frequency for which $\epsilon_g+2\epsilon_m=0$. After some algebra one finds up to first order in the fluid density n,

$$\omega\simeq\omega_0(1+n\alpha_0)\ , \tag{8}$$

where $\alpha_0=e^2f_0/m\omega_0^2\simeq 0.12$ Å^3. Thus the depolarizing field of the metal-cavity surface overcompensates the red-shifting effect of the inner Lorentz field of the bulk fluid. The net result is a blue shift of the line

$$\Delta_{2P}^{\mathrm{LR}}(\mathrm{bubble})\simeq\hbar\omega_0 n\alpha_0\simeq 2.6n\ , \tag{9}$$

measured in eV. If we try to use this formula to ac-

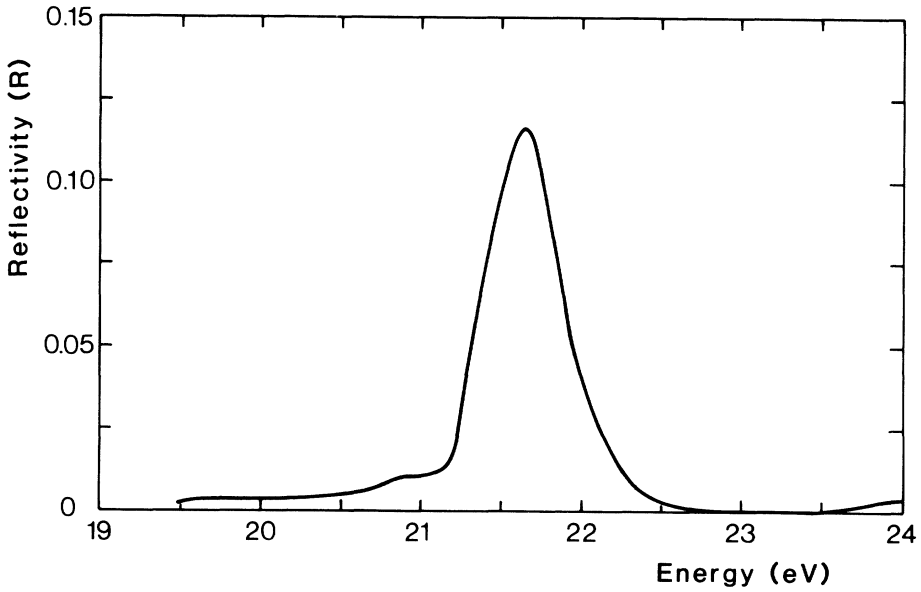

FIG. 1. Absolute reflectivity of the low-temperature liquid-He surface at near-normal incidence, as reproduced from Ref. 4.

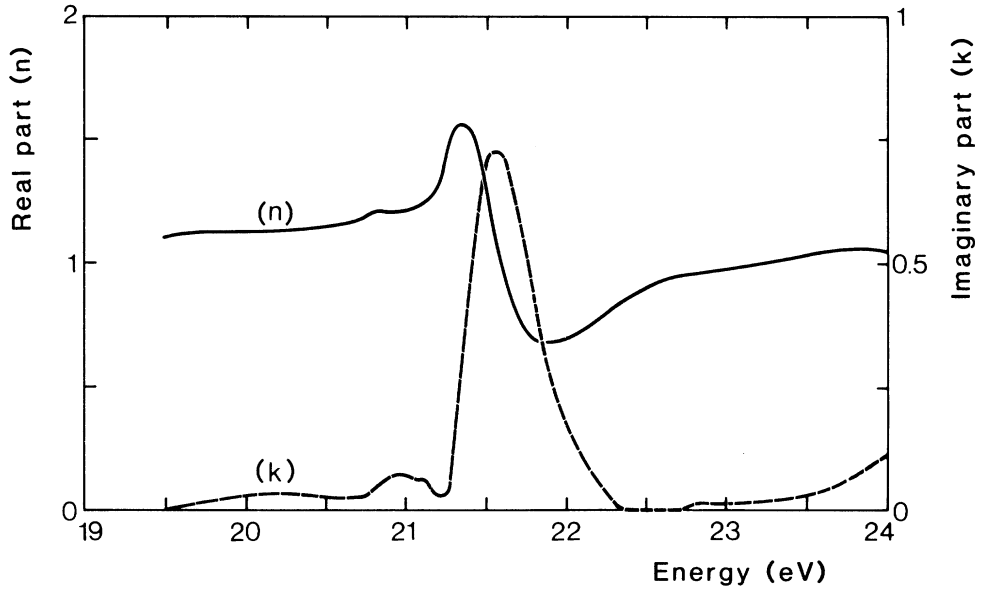

FIG. 2. Real part (n) and imaginary part (k) of the complex refractive index of liquid He obtained from a Kramers-Kronig analysis of the data in Fig. 1.

count for our observations of a 1.4-eV blue shift, we need to invoke a highly improbable density of $n \simeq 0.5$ Å^{-3} which would imply as many as 9 He atoms per Al vacancy in our bubbles. Thus the long-range (LR) dipolar effect is an order of magnitude too weak to explain our spectra. We will therefore ignore this effect in later sections.

Finally, we note that Eq. (1) evaluated at densities as high as $n \sim 0.1$ Å^{-3} (5 times the liquid density) gives a dielectric constant of order $\epsilon \simeq 1.1$ at frequencies away from resonance. Thus the empirical use of dielectric constants as high as $\epsilon \simeq 2$ by Manzke and Campagna[12] to explain some of their EELS data on He-Al thin films is difficult to justify.

III. PAULI REPULSION

It is known from both experiment and theory that the ground-state He atom repels low-energy electrons at short distances. Experimental evidences are the following:

(a) The formation of any empty cavity of some

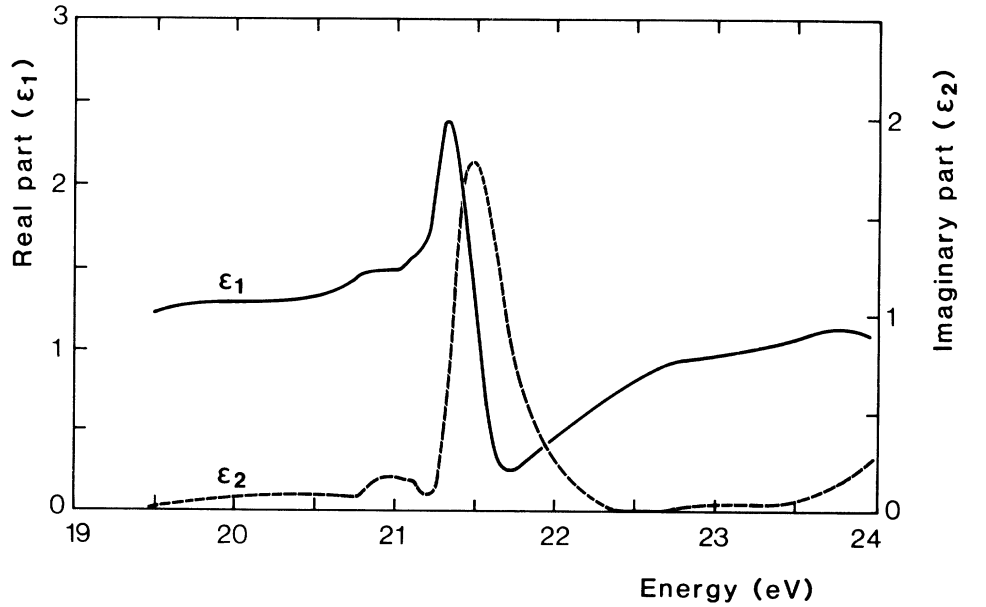

FIG. 3. Real part (ϵ_1) and imaginary part (ϵ_2) of the complex dielectric function of liquid He as obtained from a Kramers-Kronig analysis of the data in Fig. 1.

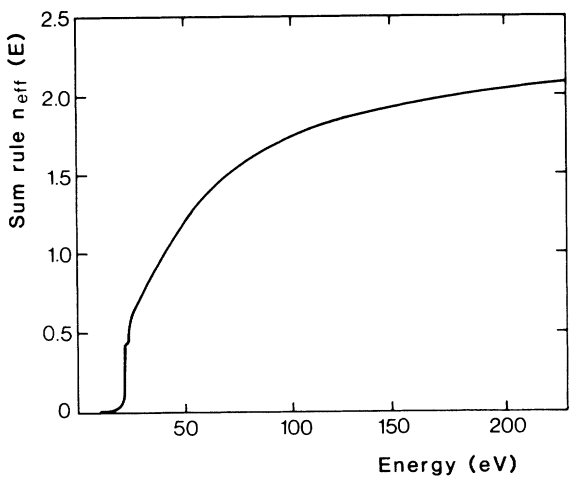

FIG. 4. Effective number of electrons taking part in absorption at energy E for liquid He as obtained from a Kramers-Kronig analysis of the data in Fig. 1. Note the correct sum-rule saturation at $n_{\text{eff}} \simeq 2$.

10–20 Å radius around a free electron injected into the dense gas, liquid, or solid He.[13,14] This is due to the fact that dense He has a positive energy barrier for free electrons which, in the liquid, is of order 1 eV. Spherical bubbles of similar size have been assumed to develop around excited He atoms[15–17] in order to understand the absorption and emission spectra of 2*S*-, 2*P*-, and 3*S*-excited atoms in liquid He.

(b) The insolubility of He in metals.[18] The conduction electrons of the metal repel the He atoms into atomic or extended traps of lowered electron density such as vacancies and voids.

Theoretically, the Pauli exclusion principle excludes occupation of the $1s^2$ closed shell of a ground-state atom by a third electron. Calculations have been performed to determine the repulsion energy for both free and bound electrons:

(1) With the use of general pseudopotential theory,[19] Kestner and co-workers[20,21] have calculated the pseudopotential repulsion experienced by a free electron from a ground-state He atom. For electrons of vanishing kinetic energy the pseudopotential energy barrier has a height of 8 eV at 1.2 a.u. from the nucleus. Averaged over the liquid, this energy barrier is of order 1 eV, in agreement with Sommers's experiment[22] which requires a barrier of 1.3 eV.

(2) Potential energy curves for the He_2^* excimer molecule in Π and Σ states have been calculated by Browne[23] and by Guberman and Goddard III,[24] respectively. Figure 5 reproduces the $D^1\Sigma_u$ molecular excited state[24] which corresponds, at large internuclear separation R, to one atom in the 1^1S_0 ground state and the other in the 2^1P_1 excited state with its $2p$ orbital along the nuclear axis. There is a positive energy shift of the excited Σ molecular level with respect to the atomic $2P$ level for all nuclear separations larger than $R \approx 1.5$ Å, a maximum close to 0.63 eV occurring around 2 Å.

Thus, on experimental and theoretical grounds, a strong electronic repulsion energy exists at a few a.u. distances from the nucleus of a ground-state He

TABLE I. Resonance-peak parameters for various optical functions as deduced from a Kramers-Kronig analysis of experimental reflectivity data of liquid He: R, reflectivity; k, imaginary part of refraction index; Imα, imaginary part of polarizability; ϵ_2, imaginary part of dielectric constant ϵ.

	Peak position (eV)	FWHM (eV)	Shift from atomic (eV)
R	21.64	0.58	0.42
k	21.57	0.47	0.35
Imα	21.61	0.43	0.39
ϵ_2	21.49	0.37	0.27

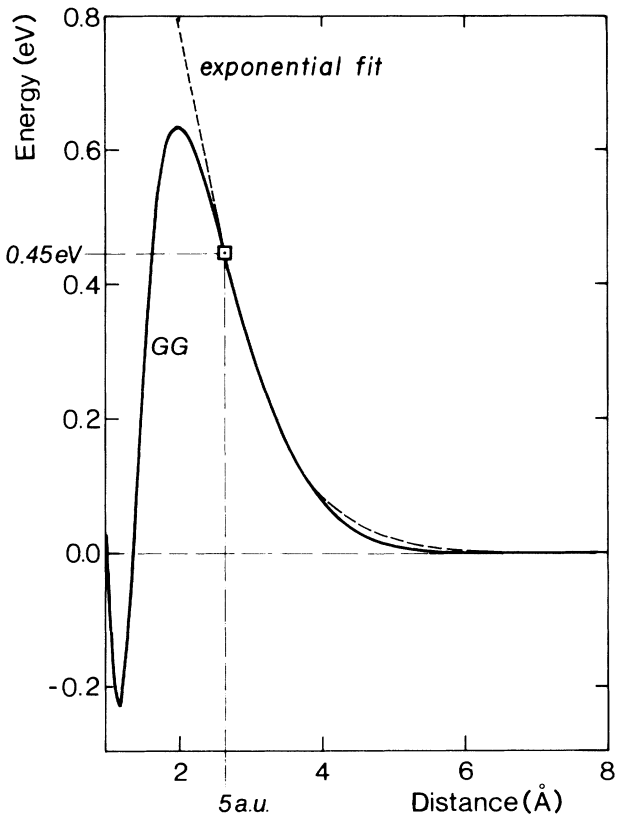

FIG. 5. Potential-energy curve for the He_2^* excimer in the $D^1\Sigma_u^+(3s\sigma,2p)$ state as reproduced from Ref. 24. The dotted curve represents the function given in Eq. (13) with $\theta=0$ (Σ state) and with C adjusted so that this function coincides with the excimer curve at the point indicated by a square.

atom. This large effect appears to be what is needed to explain our observation of the large blue shift of the absorption line in the dense fluid of our He bubbles.

A. Contact potential

For the kind of densities we are contemplating in the He fluid of the bubbles (n is approximately a few times the liquid density), the mean nearest-neighbor distance is of order $R \simeq 2$ Å. Referring to Fig. 5, this places the interatomic distances of the fluid at or beyond the maximum of the Σ excimer potential energy curve.

This part of the repulsion curve can be reproduced with reasonable accuracy by modeling the pseudopotential repulsion exerted by the ground-state He atom on the $2p$ electron of the excited atom by a simple Fermi contact potential. If we write

$$V_{\rm ps}(\vec{r}-\vec{R}) = C\delta(\vec{r}-\vec{R}) , \tag{10}$$

where the strength C is to be determined, it is straightforward to obtain the perturbation of the $2P$ state. The fact that the van der Waals energy of the He_2 molecule in its ground state is negligible for $R \geq 2$ Å indicates that the $1s$ orbital is essentially unperturbed.[24,25] We can therefore identify the blue shift of the $1S \rightarrow 2P$ absorption line of the He_2 molecule to the perturbation brought about by (10) to the $2P$ atomic level. In first order, this is

$$\Delta_2(R) = \langle 2P \mid V_{\rm ps}(\vec{r}-\vec{R}) \mid 2P \rangle = C \mid \Psi_{2P}(\vec{R}) \mid^2 , \tag{11}$$

where $\Psi_{2P}(\vec{R})$ is the normalized $2p$-orbital amplitude at $\vec{R}$. With the use of the Slater-type orbital this is

$$\Psi_{2P}(\vec{r}) = \frac{1}{\sqrt{32\pi}} \alpha^{5/2} \vec{R}^{\,0} \cdot \vec{r} e^{-(\alpha/2)r} . \tag{12}$$

$\vec{R}^{\,0}$ is the unit vector $\vec{R}/R$ along the nuclear axis and $\alpha = Z_{2p}/a_0$ is the orbital exponent with a_0 the Bohr radius and $Z_{2p} = 0.97$, the variational effective core charge as seen by the $2p$ electron.[26] Inserting (12) into (11) we get

$$\Delta_2(R,\theta) = C \frac{\alpha^5}{32\pi} R^2 \cos^2\theta e^{-\alpha R} , \tag{13}$$

where θ is the angle between the $2p$ orbital and the nuclear axis.

In Ref. 2 the constant C was chosen such as expression (13) with $\theta = 0$ fits the repulsion energy of the $D\,^1\Sigma_u^+$ state as calculated by Guberman and Goddard III[24] at some value of R in the tail of the potential-energy curve. As illustrated in Fig. 5 (dashed curve), choosing $R = 5$ a.u. gave a satisfactory fit over the entire large-R tail. This state was selected for the fit and not the $^1\Sigma_g^+(3p\sigma,2p)$ (Ref. 24) since the dipole selection rule for absorption from the gerade ground state requires an ungerade-orbital final state. The result of the fit is

$$C = 40 , \tag{14}$$

measured in eV Å^3.

We note that this value of the strength is not inconsistent with the following independent evidences concerning He:

(a) The scattering length l of He for low-energy electrons is close to 1.2 a.u.[27] The total cross section[28] of the model potential (14) being $m^2C^2/\pi\hbar^4 = 4\pi l^2$, the strength C which corresponds to the observed scattering length is found to be $C \simeq 30$ eV Å^3, i.e., reasonably close to the first estimate in Eq. (14).

(b) As noted before, liquid He presents a positive energy barrier of order $E = 1.3$ eV for electrons.[22] If we calculate the expectation value of the perturbation due to a distribution of scatterers such as (10) with respect to an electron plane wave of vanishing kinetic energy, we find $\langle E \rangle = nC$ where n is the density of scatterers. For liquid He, $n = 0.0217$ Å^{-3} and thus $C \simeq 60$ eV Å^3, again not unreasonably far from the value in (14) (if we use the theoretical estimates of $E \simeq 1$ eV from Jortner *et al.*[21] and from Burdick,[29] one gets $C \simeq 50$ eV Å^3).

The first-order perturbation energy (13) is pairwise additive. In the dense fluid environment, we can take the statistical average of this formula over all pair orientations θ and distances R. The fluid shift is then

$$\Delta_{2P} = \sum_{\vec{R}_i} \langle 2P \mid V_{\rm ps}(\vec{r}-\vec{R}_i) \mid 2P \rangle_{\rm av} = n \int d\vec{R}\, \Delta_2(R,\theta) g(R) , \tag{15}$$

where $g(R)$ is the radial pair distribution function (RPDF) of the fluid at the density and temperature of the absorption experiment. Introducing (13) into (15) and performing the angular integration gives

$$\Delta_{2P} = Cn \frac{\alpha^5}{24} \int_0^\infty dR\, R^4 g(R) e^{-\alpha R} . \tag{16}$$

In the qualitative evaluation of Ref. 2 $g(R)$ was taken to be a simple step function at some value of R:

$$g(R) = \begin{cases} 0 & \text{for } R < \sigma \\ 1 & \text{for } R \geq \sigma, \end{cases} \tag{17}$$

where $\sigma = 2.566$ Å was chosen as the distance at which the He_2 potential energy of the ground state vanishes. The remaining integration in (16) is then

elementary and the result is

$$\Delta_{2P}=Cn\frac{(\alpha\sigma)^5}{24}\int_1^\infty dx\, x^4 e^{-\alpha\sigma x}\,, \tag{18}$$

i.e., letting $u=\alpha\sigma\simeq 4.69$,

$$\Delta_{2P}=Cn(1+u+\tfrac{1}{2}u^2+\tfrac{1}{6}u^3+\tfrac{1}{24}u^4)e^{-u} \tag{19}$$

or

$$\Delta_{2P}\simeq 0.5Cn\,. \tag{20}$$

From this result and our previously determined value for C in (14), the observation of a 1.4-eV blue shift in the 1.45 at.% He sample is indicative of a density $n=0.07$ Å^{-3}.

To build confidence in this result, it is necessary to test Eq. (20) against some experimental data point. Such a test should be provided by the measured low-T liquid blue shift discussed in Sec. II. With the use of $n=0.0217$ Å^{-3} for the liquid density at 1 K, Eq. (20) gives a shift $\Delta_{2P}\simeq 0.43$ eV, not unreasonably different from the observed value in Imα (Table I). Conversely, if we start from the liquid shift in Imα to determine the strength C from Eq. (20), one finds $C\simeq 36$ eV Å^3 which then implies a density equal to $n=0.078$ Å^{-3} in the bubbles of the sample under consideration.

From the equation of state of high-density He as recently measured by Mills *et al.*[30] the above densities correspond, at room temperature, to pressures of 17 ($n=0.07$ Å^{-3}) to 24 kbar ($n=0.078$ Å^{-3}). Thus, according to this analysis, the bubbles in this particular sample are overpressurized to two or three times the surface tension pressure of 8 kbar ($4\gamma/d$ with $\gamma\simeq 1000$ erg/cm^2 and $d\simeq 50$ Å).

Before Eq. (20) can be used throughout the density range and with other He-metal systems, it is important to refine the statistical model by using in Eq. (15) the actual excimer pair interaction[24] $\Delta_2(R,\theta)$ and a more realistic pair distribution function $g(R)$, instead of the simplified ansatz of Eqs. (10) and (17). We shall find that such improvements of the model do modify appreciably the density blue-shift relationship and thus point to the importance of using an adequate statistical treatment of the high-pressure fluid.

B. Low-temperature liquid

The RPDF $g_{\text{expt}}(R)$ for liquid He has recently been accurately measured by neutron and x-ray diffraction over a range of pressures and temperatures below 4.27 K by Svensson *et al.*[31] and Robkoff and Hallock.[32] The experimental result is shown in Fig. 6 where g_{expt} is seen to vary only slightly with temperature in this range. With this basic data, we can test whether the observed liquid blue shift of Table I

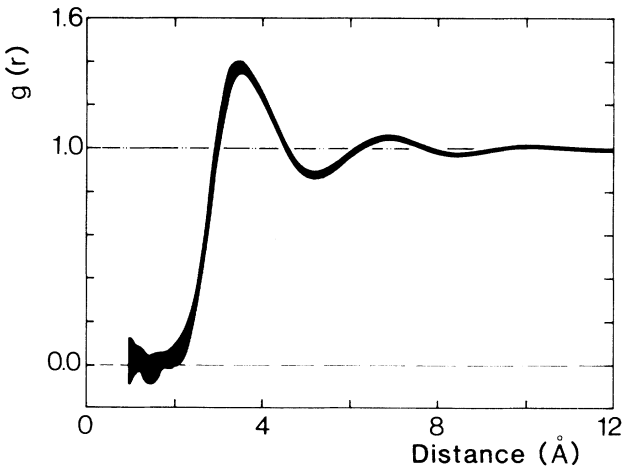

FIG. 6. RPDF of liquid He as reproduced from Ref. 30.

can be reproduced or not by the theoretical excimer curve $\Delta_2^{GG}(R)$ shown in Fig. 5. We write

$$\Delta_{2P}=n\int d\vec{R}\,\Delta_2(R,\theta)g_{\text{expt}}(R)\,, \tag{21}$$

and for $\Delta_2(R,\theta)$ we now use

$$\Delta_2(R,\theta)=\cos^2\theta\Delta_2^{GG}(R)\,. \tag{22}$$

The $\cos^2\theta$ factor which is exact for a δ-function pseudopotential as seen in Eq. (13) is meant to take account of the dependence of the excimer curve on the $2p$-orbital orientation.[33] Being zero for the Π configuration, this factor probably *underestimates* somewhat the angular averaging in Eq. (21) and hence will result in providing a *lower bound* for Δ_{2P}. This angular averaging is again trivial and the remaining radial integration has been done numerically with the result

$$\Delta_{2P}=\frac{4\pi}{3}n\int_0^\infty dR\,R^2\Delta_2^{GG}(R)g_{\text{expt}}(R)\simeq 16.6n\,, \tag{23}$$

i.e., $\Delta_{2P}\simeq 0.36$ eV at the 1-K liquid density. This is within less than 10% of the observed shift in Imα reported in Table I. Thus the use of the actual pair distribution function and theoretical excimer curve leads to a remarkable agreement between the theoretical shift and the shift deduced from reflectivity measurements.

C. Room-temperature bubbles

We now turn to the theoretical evaluation of the shift in the high-density fluid of the bubbles. We must evaluate Eq. (15). For $\Delta_2(R,\theta)$ we keep the excimer form of Eq. (22). Unfortunately, no experimental data for $g(R)$ are available at high tempera-

TABLE II. Hard-sphere diameters $d(n,t)$ which, at the indicated temperature and density, minimize the excess Helmholtz free energy given in Eqs. (25)–(28) in the text.

T (K) \ n (Å^{-3})	0.02	0.04	0.06	0.08	0.10	0.12	0.14
60	2.4300	2.3965	2.3342	2.2574	2.1784	2.1033	2.0346
120	2.2829	2.2511	2.2015	2.1416	2.0785	2.0165	1.9578
180	2.1996	2.1692	2.1252	2.0729	2.0176	1.9625	1.9096
240	2.1411	2.1117	2.0712	2.0236	1.9732	1.9226	1.8738
300	2.0957	2.0672	2.0291	1.9850	1.9381	1.8909	1.8454

tures and pressures. We must therefore rely on some theoretical RPDF. We chose to use the solution of the Percus-Yevick equation for a gas of noninteracting hard spheres.[25] Our justification for using this model, besides the great computational convenience it offers, stems from important works recently published on high-pressure helium. First, the experimental (P,V) equation of state up to 20 kbar has been obtained by Mills *et al.*[30] and the room-temperature melting point near 120 kbar has also been determined.[34] Second, these and earlier results were used as a firm thermodynamic experimental basis by Young, McMahan, and Ross[34] from which to construct an accurate theoretical equation of state for both the fluid and the solid under high and extreme pressures (up to metallization).

We shall summarize the argument of Young *et al.*[34] for the fluid phase since it is relevant for the justification of our own statistical treatment of the He bubbles. The equation of state

$$P(V,T)=-\frac{\partial}{\partial V}A(V,T) \tag{24}$$

requires a theoretical expression for the Helmholtz free energy A of the fluid. This is written as the perfect gas free energy plus an excess free energy $A_{\rm ex}$ per atom given by ($V=N/n$, where N is the number of atoms)

$$\frac{A_{\rm ex}(n,T)}{Nk_BT}=A_{\rm HS}+A_{\rm int}+A_Q\ , \tag{25}$$

where

$$A_{\rm HS}=\frac{4\eta-3\eta^2}{(1-\eta)^2}-\left[\frac{\eta^4}{2}+\eta^2+\frac{\eta}{2}\right], \tag{26}$$

$$A_{\rm int}=12\eta\int_1^\infty \Phi(x)g(x,\eta)x^2dx\ , \tag{27}$$

$$A_Q=\eta\int_1^\infty F(x)g(x,\eta)x^2dx\ . \tag{28}$$

$\eta=(\pi/6)nd^3$ is the packing fraction of the fluid of hard spheres (HS) with diameter d. The first term (26) represents an accurate analytical expression for the hard-sphere excess free energy.[34] The second term (27) in which $x=r/d$ represents the perturbation due to the interaction between the He atoms simulated by the exp(−6) potential

$$\Phi(r)=\frac{\epsilon}{k_BT}\frac{6}{a-6}\left[e^{a(1-r/r^*)}-\frac{a}{6}\left[\frac{r^*}{r}\right]^6\right], \tag{29}$$

with the following values of the parameters: $\epsilon/k_B=10.8$ K, $r^*=2.9673$ Å, $a=13.1$. The last term (28) is a quantum correction, important for He even at high temperature and pressure,[25,34] in which

$$F(r)=\frac{\Lambda^2}{2\pi}\nabla^2\Phi(r)\ , \tag{30}$$

where $\Lambda=h/\sqrt{2\pi mk_BT}$ measures the de Broglie wavelength of the He atoms of mass m and energy $\simeq k_BT$. In Eqs. (27) and (28), $g(r,\eta)$ was taken to be the Percus-Yevick hard sphere RPDF for which there exist several fast computational schemes. In our work we have used the algorithm given by Perram,[35] which is particularly efficient. A few sample g curves are given in Fig. 7 as illustrations for packing fractions η of interest in our problem.

To determine the hard-sphere diameter d appropriate to each density n and temperature T, the scheme of Young *et al.*[34] consists in minimizing the excess free energy (25) with respect to d. The a parameter in Eq. (29) is then set (at the indicated value) so as to give the overall best fit of the experimental pressure-density isotherms of helium. In order to obtain the $d(n,T)$ values relevant to our bubble problem, we have repeated this minimization scheme. Table II illustrates some of the results.[36] The scheme then completely determines, through the packing fraction η, which RPDF $g(n,T)$ should be used to evaluate the theoretical blue shift in Eq. (15) at given density and temperature. The use of a realistic RPDF brings two important improvements with respect to the simple step-function estimate of Eqs. (17) and (18):

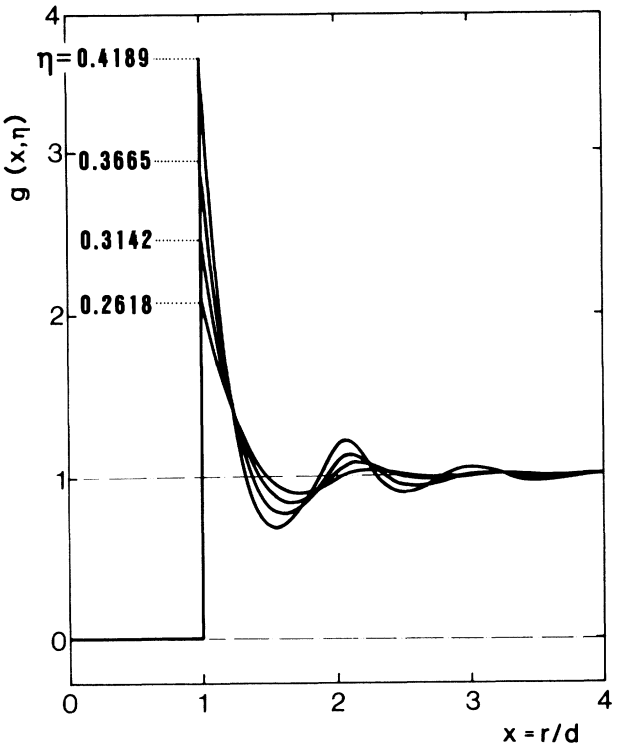

FIG. 7. RPDF as predicted by the Percus-Yevick equation for hard spheres of diameter d. η is the packing fraction parameter related to density n by $\eta=\pi n d^3/6$.

(i) The average nearest-neighbor distance d in the model dense fluid depends on density and temperature as it should, whereas in Eq. (17), d was set at the fixed value $\sigma=2.566$ Å (to be compared with d values of order 2 Å in Table II).

(ii) The structure of the fluid is taken into account through the oscillations of the RPDF, while in Eq. (17) complete randomness was assumed.

The end result for the blue-shift function $\Delta_{2P}(n,T)$ is given in Table III. Figure 8 shows the predicted $\Delta_{2P}(n)$ at room temperature. The shift is seen to be nearly linear in the density range shown and only weakly temperature dependent. A linear fit of the 300-K curve from $n=3\times10^{22}$ cm^{-3} to $n=7\times10^{22}$ cm^{-3} is

$$\Delta_{2P}(\text{eV})=31n(\text{Å}^{-3})-0.15\ , \qquad (31)$$

measured in eV, which should be compared with our previous estimate in Eq. (20), i.e., $\Delta_{2P}=20\ n$ (using $C=40$ eV Å^3). The slope in (31) is substantially higher than in the simplified model. This mainly comes from the fact that the Percus-Yevick RPDF starts at $d\simeq2$ Å, whereas the step RPDF used in Eqs. (21) and (18) started only at $\sigma=2.556$ Å and hence the result (31) includes higher values of the excimer blue shift than (20).

TABLE III. Blue-shift function $\Delta_{2P}(n,T)$, as predicted by Eq. (15), as a function of temperature and density.

T (K) \ n (Å^{-3})	0.03	0.04	0.05	0.06	0.07	0.08	0.09	0.10	0.11	0.12	0.13	0.14
60	0.743 (eV)	1.053	1.382	1.724	2.072	2.420	2.766	3.107	3.440	3.764	4.075	4.375
140	0.778	1.084	1.405	1.737	2.074	2.414	2.752	3.086	3.415	3.737	4.051	4.354
220	0.795	1.099	1.417	1.744	2.076	2.410	2.744	3.074	3.400	3.718	4.030	4.336
300	0.806	1.110	1.425	1.749	2.078	2.408	2.738	3.064	3.387	3.705	4.016	4.321

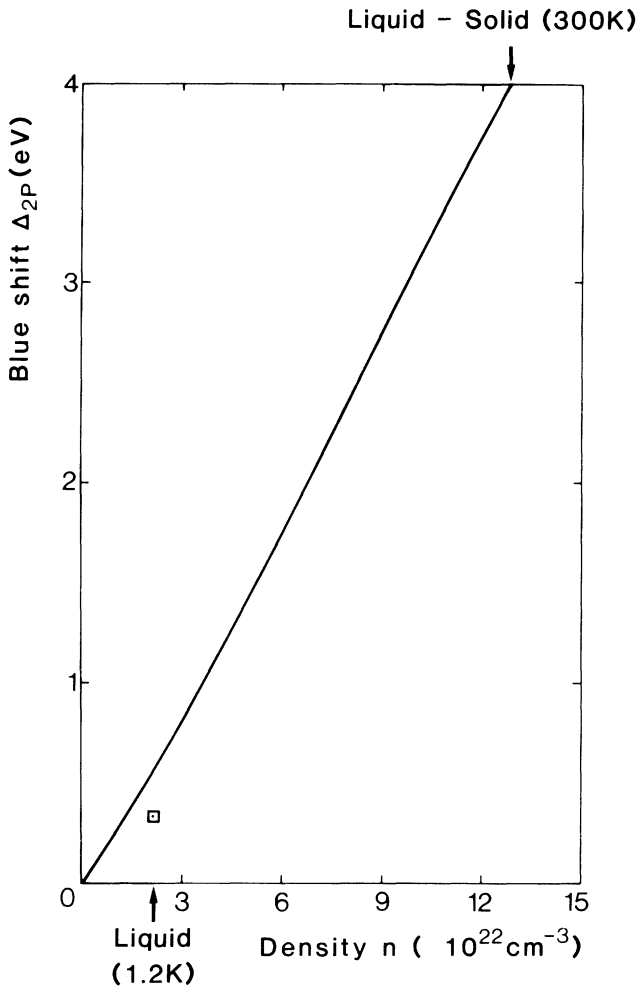

FIG. 8. Blue-shift function of the resonance line of He as a function of gas density, at room temperature. The square indicates the shift for low-T liquid observed from reflectivity data.

It is seen from Table III or Fig. 8 that our observed blue shift of 1.4 eV in the 50-Å bubbles now implies a density of $n=0.05$ Å^{-3}. From the $P(n,T)$ isotherm at $T=300$ K,[34] this density corresponds to a pressure of $P\simeq 7$ kbar which should be compared to the surface-tension pressure of $P=2\gamma/r=8$ kbar for $r=25$ Å in aluminum ($\gamma\simeq 1000$ erg/cm^2). We conclude that in this particular sample and according to the presently improved statistical model, the bubbles should be in near equilibrium, contrary to what was concluded from the simpler model in Sec. III A, where overpressurized bubbles were implied. In the 3.1 at % He samples, the observed 2-eV shift appears to indicate a density of $n\simeq 7\ 10^{22}$cm^{-3}, i.e., a pressure of $P=16.5$ kbar.[34] Equilibrium bubbles with this pressure would have a diameter of 24 Å. The sample showed a large population of 40-Å-diam bubbles plus a broad tail towards larger ones up to 200-Å diameter. Thus it seems that this heavily implanted sample contains a majority of overpressurized bubbles.

IV. LINE SHAPE

We wish to investigate in this section whether the Pauli repulsion effect, which seems capable of accounting for the line shifts, is also consistent with the observed widths. We start from Anderson's line-shape formula,[37] which predicts a line intensity

$$I(\omega)=\int_{-\infty}^{+\infty} d\tau e^{i\omega\tau}C(\tau)\ , \tag{32}$$

equal to the Fourier transform of the correlation function ($\hbar=1$),

$$C(\tau)=\exp\left[-n\int d\vec{R}(1-e^{-i\tau\Delta_2(\vec{R})})g(R)\right]\ . \tag{33}$$

Again pairwise additivity of the energy shift function $\Delta_2(\vec{R})$ of the He_2^* excimer is assumed to hold. Moreover, the correlation function (33) holds true only in the static limit, certainly valid here, where the atoms can be considered as immobile during the $1S\rightarrow 2P$ absorption event.

If we expand the exponential in small parentheses in powers of Δ_2 we obtain, up to second order,

$$\begin{aligned} I(\omega)&=\int_{-\infty}^{+\infty} d\tau e^{i\omega\tau}\exp(-i\tau\Delta_{2P}-\tfrac{1}{2}\tau^2\Gamma^2) \\ &=\sqrt{\pi}\exp\left[\frac{(\omega-\Delta_{2P})^2}{-2\Gamma^2}\right], \end{aligned} \tag{34}$$

where

$$\Delta_{2P}=n\int d\vec{R}\,\Delta_2(\vec{R})g(R) \tag{35}$$

gives the line shift, as before, e.g., in Eq. (15), and where

$$\Gamma^2=n\int d\vec{R}[\Delta_2(\vec{R})]^2 g(R)\ . \tag{36}$$

Thus, to this order, the line shape is Gaussian and of width (FWHM):

$$W=2\sqrt{2\ln 2}\,\Gamma=2.35\Gamma\ . \tag{37}$$

The same computer code which generated Δ_{2P} in Eq. (35) from the theoretical excimer shift $\Delta_2^{GG}(R)$ can also produce the width function Γ. The result is shown in Table IV for the investigated range of densities. The width is remarkably well accounted for in the 1.5 at. % sample ($n=5$) which, we will recall, has a fairly uniform size distribution around 50 ± 10 Å. The discrepancy between observed and calculated widths for the 3.5 at. % sample ($n=7$) may be partly due to the much more irregular size distribution of the bubbles, which probably entails a distribution of density values.

TABLE IV. Gaussian linewidth (FWHM) predicted by static line-broadening theory as a function of density and at room temperature. The line marked "liquid" concerns the low-T liquid results. The densities $n=5\times10^{2}$ cm^{-3} and $n=7\times10^{22}$ cm^{-3} are obtained by fitting the theoretical blue shifts to the indicated observed ones. All theoretical widths are calculated from the indicated theoretical shifts.

	Shift Δ_{2P} (eV)		Width W (eV)	
n (10^{22} cm^{-3})	Experimental fit	Theory	Experimental fit	Theory
2		0.52		0.75
2.17 (liquid)	0.39	0.36	0.43	0.53
3		0.80		0.95
4		1.11		1.13
5	1.40	Fitted	1.2	1.30
6		1.75		1.45
7	2.0	Fitted	2.2	1.60
8		2.41		1.74
9		2.74		1.87
10		3.06		1.99

For the low-temperature liquid, the theoretical width has been evaluated from (36) but with $g(R)=g_{\text{expt}}(R)$ as in (21) rather than with the Percus-Yevick g, which is unreliable at low temperature and with $\Delta_2(R)$ as given by Eq. (22). Thus we have for the liquid.

$$\Gamma^2=\frac{4\pi}{5}n\int_0^\infty dR\,R^2[\Delta_2^{GG}(R)]^2 g_{\text{expt}}(R)\,, \qquad (38)$$

and we found $\Gamma^2=0.05$ eV^2, hence a width $W=0.53$ eV. Although this result at first appears reasonably close to the observed width (0.43 eV, see Table I), the remaining 20% discrepancy exceeds the experimental uncertainty from the reflectivity data and from the liquid $g_{\text{expt}}(R)$.

This points to the need of a theoretical reevaluation of the excimer potential-energy curve on which we rely for our calculations of the liquid line shift and width in Eqs. (23) and (38). Such a reevaluation is also desirable for the interpretation of the bubble data, particularly in view of the fact that the predicted line-shape parameters in that case depend critically on the height of the hump around 2 Å in the excimer curve. Work is in progress in this direction.

ACKNOWLEDGMENTS

This work was supported by the Belgian Ministry of Science Policy, the Royal Society in the form of a European Science Exchange Programme fellowship (S.E.D.), and North Alantic Treaty Organization Research Grant No. 1970 (S.E.D., J.C.R.).

[1]S. E. Donnelly, J. C. Rife, J. M. Gilles, and A. A. Lucas, J. Nucl. Mater. 93-94, 767 (1980).
[2]J. C. Rife, S. E. Donnelly, A. A. Lucas, J. M. Gilles, and J. J. Ritsko, Phys. Rev. Lett. 46, 1220 (1981).
[3]S. E. Donnelly, J. C. Rife, J. M. Gilles, and A. A. Lucas, IEEE Trans. Nucl. Sci. NS-28, 1820 (1981).
[4]C. M. Surko, F. J. Dick, F. Reif, and W. C. Walker, Phys. Rev. Lett. 23, 842 (1969).
[5]K. Ohtaka and A. A. Lucas, Phys. Rev. B 18, 4643 (1979).
[6]M. Lallemand and D. Vidal, J. Chem. Phys. 66, 4776 (1977).
[7]J. Ziman, *The Principles of the Theory of Solids* (Cambridge University Press, Cambridge, 1972).
[8]M. H. Edwards, Can. J. Phys. 36, 884 (1958).
[9]J. A. R. Sampson, J. Opt. Soc. Am. 54, 876 (1964); Phys. Rev. Lett. 22, 693 (1969).
[10]G. G. Grandqvist and O. Hunderi, Phys. Rev. B 16, 3513 (1977).
[11]H. J. Hageman, W. Gudat, and C. Kunz, Deutsche Elektronen-Synchrotron Report No. SR-74/7 (unpublished).
[12]R. Manzke and M. Campagna, Solid State Commun. 39, 313 (1981).
[13]J. Levine and T. M. Sanders, Phys. Rev. Lett. 8, 159 (1962).
[14]K. W. Schwarz, Phys. Rev. B 21, 5125 (1980).
[15]F. J. Soley and W. A. Fitzsimmons, Phys. Rev. Lett.

32, 988 (1974).
[16]W. Steets, A. P. Hickman, and N. F. Lane, Chem. Phys. Lett. 28, 31 (1974).
[17]J. Wisdom, T. W. Hartquist, and N. F. Lane, Phys. Rev. B 14, 4205 (1976).
[18]J. E. Inglefield and J. B. Pendry, Philos. Mag. 34, 205 (1976); R. Benedek, J. Phys. F 8, 5 (1978).
[19]B. J. Austin, V. Heine, and L. J. Sham, Phys. Rev. 127, 276 (1962).
[20]N. R. Kestner, J. Jortner, M. H. Cohen, and S. A. Rice, Phys. Rev. 140, A56 (1965).
[21]J. Jortner, N. R. Kestner, S. A. Rice, and M. H. Cohen, J. Chem. Phys. 43, 2614 (1965).
[22]W. T. Sommers, Phys. Rev. Lett. 12, 271 (1964).
[23]J. C. Browne, Phys. Rev. 138, A9 (1965).
[24]S. L. Guberman and W. A. Goddard III, Phys. Rev. A 12, 1203 (1975).
[25]J. A. Barker and D. Henderson, Rev. Mod. Phys. 48, 587 (1976).
[26]H. A. Bethe and E. E. Salpeter, in *Handbuch der Physik XXXV, Atome I,* edited by H. Geiger and K. Scheel (Springer, Berlin, 1957), p. 88.
[27]T. F. O'Malley, Phys. Rev. 130, 1020 (1963).
[28]D. ter Haar, *Selected Problems in Quantum Mechanics* (Academic, New York, 1964), p. 382.
[29]B. Burdick, Phys. Rev. Lett. 14, 11 (1965).
[30]R. L. Mills, D. H. Leibenberg, and J. C. Bronson, Phys. Rev. B 21, 5137 (1980).
[31]E. C. Svensson, V. F. Sears, A. D. B. Woods, and P. Martel, Phys. Rev. B 21, 3638 (1980).
[32]H. N. Robkoff and R. B. Hallock, Phys. Rev. B 25, 1572 (1982).
[33]Browne (Ref. 23) has calculated the $^1\Sigma_u$ state repulsion curve and found a large maximum of 0.6 eV at $R \simeq 1.8$ Å, i.e., similar to the $\Delta_2^{GG}(R)$ for the $^1\Sigma_u$ excimer state of Ref. 26. This rather unphysical result has been criticized by Guberman and Goddard III (Ref. 24).
[34]J. M. Besson and J. P. Pinceaux, Science 206, 1073 (1979); D. A. Young, A. K. McMahan, and M. Ross, Phys. Rev. B 24, 5119 (1981).
[35]J. W. Perram, Mol. Phys. 30, 1505 (1975).
[36]Our d values coincide with those calculated by Young *et al.* (Ref. 34) to whom we express our appreciation for sending us some of their data.
[37]P. W. Anderson, Phys. Rev. 86, 809 (1952).